MVA2005 IAPR Conference on Machine VIsion Applications, May 16-18, 2005 Tsukuba Science City, Japan
4-1

A robust active contour initialization and gradient vector flow for ultrasound image segmentation

C Tauber, H Batatia, A Ayache

IRIT-ENSEEIHT, Toulouse, France

Abstract

Speckle and low contrast make ultrasound image segmentation a difficult task. This paper presents an original robust active contour energy and the corresponding quasi-automatic initialization. Both are based on the coefficient of variation gradient vector flow. Our approach combines anisotropic diffusion with the gradient vector flow field. The gradient vector flow is calculated from a map of the amplitudes of the coefficient of variation. This makes it more robust to speckle. The centers of divergence are calculated and used to initialize the active contour model. The method has been tested on different echocardographic images. The results presented are very encouraging.

1. Introduction

Ultrasound (US) imagery is characterized by low signal to noise ratio, low contrast between tissues and speckle contamination causing erroneous detection of cavities boundaries. Active contour models (snakes) deal with some of these limitations. They consider boundaries as inherently connected smooth curves. A snake is a curve that evolves from an initial position towards the boundary of an object, minimizing some energy functional [1, 2, 3]. A B-spline snake is an energy minimizing spline parameterized by its control points. The smoothness of the snake is implicitly given by the B-spline model [4, 5, 6]. The energy consists in two terms: the internal energy and the external energy. The first affects the smoothness of the curve, and the second attracts the snake toward image features. A number of external energy terms have been proposed [7, 8, 9] . Most of these approaches either use gradient information or global image statistics. Among them the gradient vector flow field introduced by Xu [9] has the inherent property of being able to reconstruct subjective contours. These contours are edges that are not actually present in an image, but are perceived nevertheless. This characteristic is very attractive for US imagery where connected boundaries are less likely to be found. However this method cannot be used efficiently for US imaging because of the presence of speckle. A novel method for anisotropic diffusion of ultrasound images was introduced in [10]. It uses the local coefficient of variation (LCV) [11] and a robust diffusion tensor to filter echographic images. The LCV is computed locally and compared to the global coefficient of variation (GCV). In homogeneous areas affected by speckle LCV is close to GCV. Near edges LCV becomes greater. This diffusion technique was successfully used in [12] as a pre-step for segmentation of the heart cavities in US images. However this B-spline snake method is difficult to initialize. It is well known that the snake initialization accuracy influences significantly the segmentation. Using primer contour as the snake initialization have been proposed in [13, 14], multi-scale approach was proposed in [15], balloon snakes and GVF were proposed in [2, 9].

In this paper we derive a new gradient vector flow based on the amplitude of the coefficient of variation, called Speckle resistant Gradient Vector Flow (s-GVF). First we use a robust anisotropic model to filter the US image. Then we generate an image of the LCV amplitude which is used to generate the s-GVF. The s-GVF centers of divergence are used to develop a quasi-automatic curve initialization and the s-GVF is used to attract the B-spline snake toward the cavities boundaries.

The remainder of this paper is organized as follows. We present the s-GVF in section 2.1. In section 2.2 we present a new model for quasi-automatic initialization of the B-spline snake. The results are shown in section 3, and a discussion and conclusion can be found in section 4.

2. Methods

2.1. The speckle resistant gradient vector flow

To generate the s-GVF we first apply anisotropic diffusion described in [10] to generate a coefficient of variation amplitude map. The anisotropic diffusion is

performed by solving the following PDE :

$$\begin{cases} \frac{\delta I(x,t)}{\delta t} = \text{div}[g(\gamma(x,t))\nabla I(x,t)] \\ I(x,0) = I_0(x),\ \left(\frac{\delta I(x,t)}{\delta \vec{n}}\right)|_{\delta\Omega} = 0 \end{cases} \quad (1)$$

where γ is an estimation of the LCV, div stands for the divergence, ∇ denotes the gradient, $I_0(x)$ is the original image intensity of the pixel x, $\delta\Omega$ is the image domain border, $\vec{n}$ is the outward normal vector of $\delta\Omega$, and $g(\gamma)$ is the diffusion tensor defined as :

$$g(\gamma)_{i,j} = \begin{cases} \left[1 - \frac{\gamma^2(i,j;t)}{\gamma_s^2(t)}\right]^2 & \text{if } \gamma(i,j;t) \leq \gamma_s(t), \\ 0 & \text{otherwise.} \end{cases} \quad (2)$$

where $\gamma_s = \sqrt{5}\gamma_e$ and γ_e is a robust estimation of the LCV interception term :

$$\begin{aligned} \gamma_e(t) &= c \underset{(i,j)\in\Omega}{\text{med}}(|\gamma(i,j;t) - \underset{(i,j)\in\Omega}{\text{med}}(\gamma(i,j;t))|) \\ &\quad + \underset{(i,j)\in\Omega}{\text{med}}(\gamma(i,j;t) \end{aligned}$$

whith $c = 1.4826$. The diffusion stops when image $I_{i,j}^{t_e}$ is considered stationary, *i.e.* when $\gamma_e(t_e) \leq \epsilon$, a small positive threshold defined empirically. Figure 1(b) shows result of this method. We then calculate the contour image

$$I_\gamma(i,j) = \begin{cases} \gamma(i,j;t_e) & \text{if } \gamma(i,j;t_e) > \tau, \\ 0 & \text{otherwise.} \end{cases} \quad (3)$$

Figure (fig.1) (c) shows an example of such image. The gradient amplitude of the final image is used to compute the s-GVF.

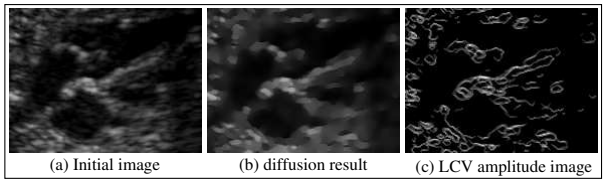

(a) Initial image (b) diffusion result (c) LCV amplitude image

Figure 1. (a) Original image. (b) Diffusion filtered image using LCV and a robust tensor[14]. (c) Thresholded LCV image

To generate the s-GVF $\text{gv}(\text{x},\text{y}) = [\text{u}(\text{x},\text{y}), \text{v}(\text{x},\text{y})]$ we use the classical GVF energy minimisation equation [9] but replace the gradient amplitude with the LCV gradient amplitude resulting from the anisotropic diffusion:

$$\text{E} = \int\int \mu(\text{u}_\text{x}^2 + \text{u}_\text{y}^2 + \text{v}_\text{x}^2 + \text{v}_\text{y}^2) + |\nabla \text{I}_\gamma|^2 |\mathbf{v} - \nabla \mathbf{I}_\gamma|^\mathbf{2} \mathbf{dxdy}. \quad (4)$$

where u_x, u_y, v_x and v_y are the partial derivative of corresponding functions and μ a regularization parameter. Discretizing using the Euler equations leads to an iterative resolution where :

$$\begin{aligned} u_{i,j}^{n+1} &= (1 - g_{i,j}^2\Delta t)u_{i,j}^n + r(u_{i+1,j} + u_{i-1,j} + u_{i,j+1} \\ &\quad + u_{i,j-1} - 4u_{i,j}) + c_{i,j}^h \Delta t \\ v_{i,j}^{n+1} &= (1 - g_{i,j}^2\Delta t)v_{i,j}^n + r(v_{i+1,j} + v_{i-1,j} + v_{i,j+1} \\ &\quad + v_{i,j-1} - 4v_{i,j}) + c_{i,j}^v \Delta t \end{aligned}$$

with :

$$\begin{aligned} g^2(x,y) &= \frac{\partial I_\gamma(x,y)}{\partial x}^2 + \frac{\partial I_\gamma(x,y)}{\partial y}^2 \\ (c^h(x,y), c^v(x,y)) &= g^2(x,y)\left(\frac{\partial I_\gamma(x,y)}{\partial x}, \frac{\partial I_\gamma(x,y)}{\partial y}\right) \\ r &= \frac{\mu\Delta t}{\Delta x \Delta y} \end{aligned}$$

Figure 2(a) presents the s-GVF of the right auricle of the US image (fig.1(a)). Using the LCV gradient instead of the intensity gradient improves the precision and stability of the field : the s-GVF is smooth and points toward the cavity boundaries without being affected by speckle.

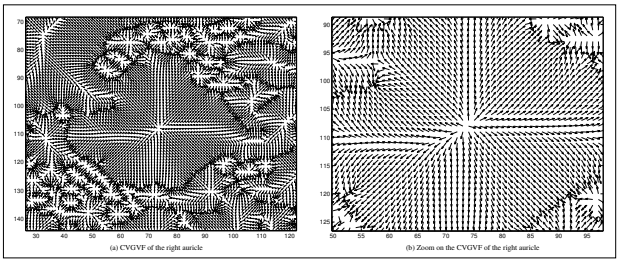

(a) CVGVF of the right auricle (b) Zoom on the CVGVF of the right auricle

Figure 2. (a) GVF of the bottom right part of the US image (b) Zoom in the right auricle cavity

2.2. Curve initialization

We propose a quasi-automatic method to initialize the snake. First we propose a generalization of the centers of divergence (CD) introduced in [16]. Let sign be a function defined as :

$$\text{sign(x)} = \begin{cases} 1 & \text{if } x > 0 \\ 0 & \text{if } x = 0 \\ -1 & \text{if } x < 0 \end{cases} \quad (5)$$

The vertical and horizontal CD are defined as

$$\begin{aligned} \mathbf{Cd_i} &= \{(i,j)|u(i,j) \leq u(i+1,j) \\ &\quad \wedge |\text{sign}(\text{u(i,j)}) + \text{sign}(\text{u(i+1,j)})| \leq 1\} \\ \mathbf{Cd_j} &= \{(i,j)|v(i,j) \leq v(i,j+1) \\ &\quad \wedge |\text{sign}(\text{v(i,j)}) + \text{sign}(\text{v(i,j+1)})| \leq 1\} \end{aligned}$$

we propose two different definitions for the CD set :

$$\mathbf{Cd}_{\text{strong}} = \{(i,j)|(i,j) \in \mathbf{Cd_i} \wedge (\mathbf{i},\mathbf{j}) \in \mathbf{Cd_j}\} \quad (6)$$

$$\mathbf{Cd}_{\text{weak}} = \{(i,j)|(i,j) \in \mathbf{Cd_i} \vee (\mathbf{i},\mathbf{j}) \in \mathbf{Cd_j}\} \quad (7)$$

As presented in [9] the GVF (respectively s-GVF) attracts the snake to the curve, even if the snake is not close to the contour to be detected. However this does not completely solve the initialization problem : if all points of the initial curve are closer to a part of the boundary, the curve is entirely attracted to it (fig.3).

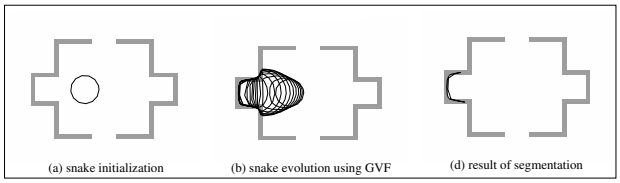

Figure 3. Exemple of a bad initialization using the GVF.

A solution is to use the CD of the s-GVF : the region delimited by the initial curve should include all the $\mathbf{Cd}_{\text{strong}}$ of the cavities and its shape skeleton should be the $\mathbf{Cd}_{\text{weak}}$ connecting those $\mathbf{Cd}_{\text{strong}}$. This is done by manual or automatic selection of a point p in the cavity, then using the inverse s-GVF to reach the closest $\mathbf{Cd}_{\text{strong}}$:

$$\text{While}(\text{p} \notin \mathbf{Cd}_{\text{strong}})\ \mathbf{p} \leftarrow \mathbf{p} - \text{gv}(\text{p}); \quad (8)$$

Once a point $p_s \in \mathbf{Cd}_{\text{strong}}$ is found, we select all the $\mathbf{Cd}_{\text{strong}}$ connected to it via $\mathbf{Cd}_{\text{weak}}$ points. We use a morphological dilatation of the connected path and extract its boundary. This is the initialization of the curve. This method benefits the closeness of weak centers of divergence to the skeleton of the objects in the image. Thus we can generate an initial curve directly related to the shape of the cavity to be detected, ensuring that all parts of the initial curve will be attracted toward different directions. Figure 4 shows an example of a snake initialization for a synthetic image.

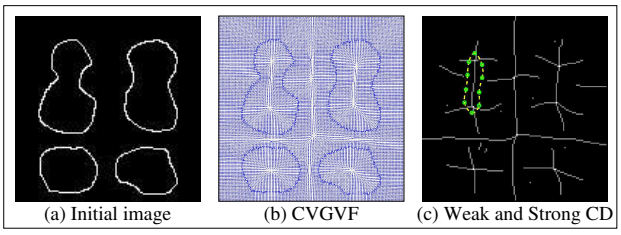

Figure 4. Weak and strong centers of divergence of a synthetic image, and the corresponding snake initialization

3. Results

The model has been applied to an ultrasound video sequence of the four cardiac chambers view of a 12 weeks old foetus [1]. We segment the right auricle which contains only one strong center of divergence. We also present the result on a US image of the same view of a grown up person [2]. In this image we segment the left ventricle which contains 2 strong centers of divergence. Both experiments use the B-spline snake algorithm presented in [12]. We use our quasi-automatic initialization presented in this paper. The s-GVF is used as a second external energy to attract the snake toward the boundaries.

Figures 5 and 6 contain 3 images : the initial image, the selected point and the initial snake, and the segmentation result. The results show that the initialization is correct and that the s-GVF is efficient to detect the heart cavities.

4. Discussion and conclusions

We have presented a new method for active contour initialization and an adaptation of the gradient vector field to images affected by speckle. Unlike other approaches, the s-GVF uses the local coefficient of variation (LCV) to improve robustness to speckle. The method proposed is quasi-automatic as it requires the selection of one point inside the cavity. When applying the method over a video sequence, it is possible to use the centre of gravity of the final curve as the next frame initialization. The experimental results on echocardiographic images are very encouraging. This method is being used to develop a novel robust method to segment echographic images affected by speckle.

References

[1] Kass M, Witkin A, Terzopoulos D. Snakes: Active contour models. Int J Comput Vis 1988;1:321–332.

[2] Cohen L. On active contour models and balloons. Computer vision graphics and image processing Image Understanding 1991;53:211–218.

[3] Delingette H, Hebert M, Ikeuchi K. Shape representation and image segmentation using deformable surfaces. IEEE Proceedings of Computer Vision and Pattern Recognition 1991;467–472.

[4] Menet S, Saint-Marc P, Medioni G. B-snakes: Implementation and application to stereo. Proc Image Understanding Workshop 1990;720–726.

[5] Brigger P, Hoeg J, Unser M. B-spline snakes: A flexible tool for parametric contour detection. IEEE Trans Image Processing 2000;9:1484–1496.

[6] Jacob M, Blu T, Unser M. Efficient energies and algorithms for parametric snakes. IEEE Trans on Image Processing 2004;13:1231–1244.

[7] Klein A, Egglin T, Pollak J, Lee F, Amini A. Identifying

[1] We thank Dr Bereni and the Clinique de Notre Dame de Perpignan for providing us the images

[2] We thank Universita di Bologna for providing us the images

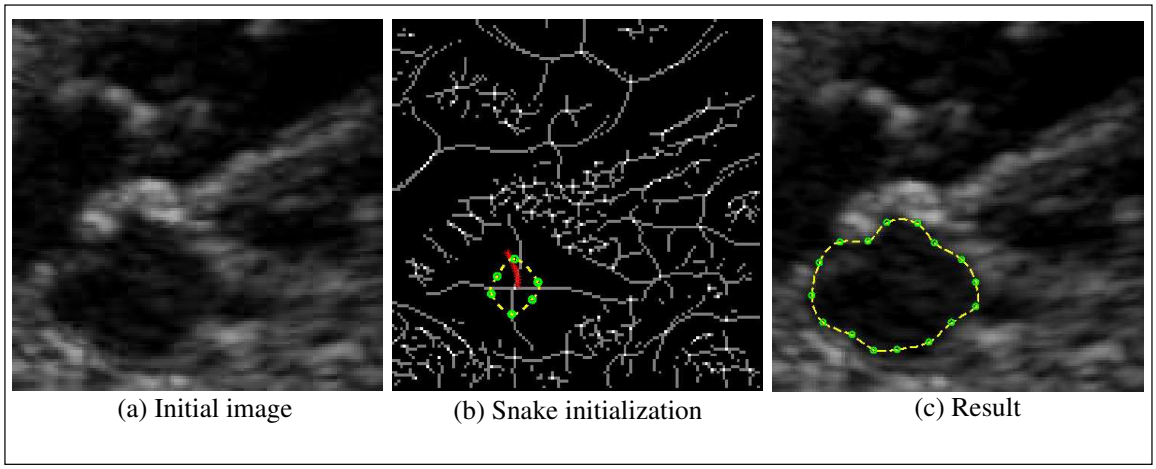

(a) Initial image (b) Snake initialization (c) Result

Figure 5. Detection of an auricle containing one strong center of divergence.

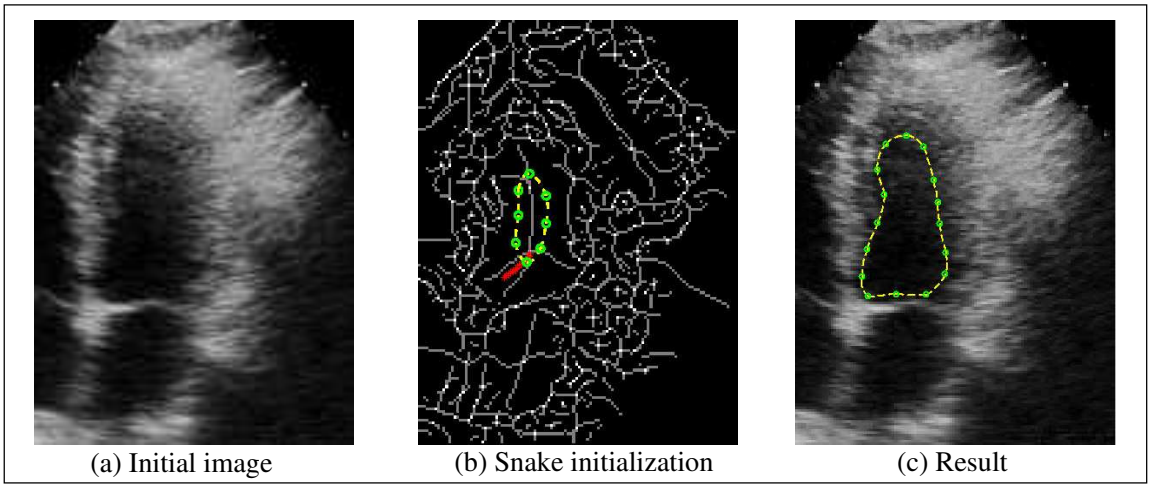

(a) Initial image (b) Snake initialization (c) Result

Figure 6. Detection of a ventricle containing two connected strong centers of divergence.

vascular features with orientation specific filters and b-spline snakes. Computers in Cardiology 1994;113–116.

[8] Berger MO, Maurice N, Winterfeldt G, Lethor JP. Automatic 3d reconstruction of the beating left ventricle using transthoracic echographic images. Computers in Cardiology 1998;641–644.

[9] Xu C, Prince J. Snakes, shapes, and gradient vector flow. IEEE Trans on Image Proc 98;7:359–369.

[10] Tauber C, Batatia H, Ayache A. A robust speckle reducing anisotropic diffusion. Proceedings of IEEE International Conference on Image Processing ICIP to appear 2004;.

[11] Yu Y, Acton S. Speckle reducing anisotropic diffusion. IEEE Trans on Image Proc 2002;11:1260–1270.

[12] Tauber C, Batatia H, Morin G, Ayache A. Robust b-spline snakes for ultrasound images segmentation. IEEE Computers in Cardiology Chicago to appear 2004;.

[13] Raganath S. Contour extraction from cardiac mri studies using snakes. IEEE Transactions on Medical Imaging 1995; 14:328–338.

[14] Kichenesamy S, Kumar A, Olver P, Tannenbaum A, Yezzi A. A geometric snake model for segmentation of medical imagery. IEEE Transactions on Medical Imaging 1997; 16:199–209.

[15] Mignotte M, Meunier J. An unsupervised multiscale approach for the dynamic contour-based boundary detection issue in ultrasound imagery. CVPRIP00 2000; 2:366–369.

[16] Xingfei G, Tian J. An automatic active contour model for multiple objects. Pattern Recognition 2002 Proceedings 16th International Conference on 2002;2:881–884.

Address for correspondence:
Clovis Tauber
2 rue camichel, BP7122. 31071 Toulouse Cedex 7, France
tauber@enseeiht.fr